The Depositional Record
The journal of the International Association of Sedimentologists
Open Access

ORIGINAL RESEARCH ARTICLE

Lowstand wedges in carbonate platform slopes (Quaternary, Maldives, Indian Ocean)

CHRISTIAN BETZLER*, CHRISTIAN HÜBSCHER†, SEBASTIAN LINDHORST*, THOMAS LÜDMANN*, JOHN J. G. REIJMER‡ and JUAN-CARLOS BRAGA§

*Institut für Geologie, CEN, Universität Hamburg, Bundesstrasse 55, 20146 Hamburg, Germany (E-mail: christian.betzler@uni-hamburg.de)
†Institut für Geophysik, CEN, Universität Hamburg, Bundesstrasse 55, 20146 Hamburg, Germany
‡King Fadh University of Petroleum & Minerals, KFUPM Box 2263, Dhahran 31261, Saudi Arabia
§Departamento de Estratigrafía y Paleontología, Universidad de Granada,Campus de Fuentenueva s.n., 18002 Granada, Spain

Keywords
Drift deposits, large benthic foraminifers, rhodoliths, sea-level, sequence stratigraphy.

Manuscript received: 6 September 2016; Accepted: 26 October 2016

The Depositional Record 2016; 2(2): 196–207

doi: 10.1002/dep2.21

ABSTRACT

Seismic, hydroacoustic and sedimentological data were used to analyse the response of atoll-slope sedimentation in the Maldives to the late Quaternary sea-level change. The slope deposits, as imaged in multichannel seismic profiles, are arranged into stacked aggrading to backstepping basinward thinning wedges. In a piston core recovered at the lower slope of one of the atolls, the sediment texture ranges from packstone to rudstone. Major components are blackened bioclasts, the large benthic foraminifers *Operculina* and *Amphistegina*, together with *Halimeda* debris and red algae. Radiocarbon dating at a core depth of 66 cm indicates that the wedge sedimentation stopped or was largely reduced after 16 ka BP. Therefore, the atoll-slope deposits largely consist of sediment formed *in situ* and deposited during the last glacial lowstand in sea-level. This is in apparent contradiction to the concept of highstand shedding of tropical carbonate platforms, which requires slope sedimentation during sea-level highstands, when the platform is flooded. Rather than intrinsic factors, such as sediment bypass along the steep slope, the extrinsic process of current winnowing of the slope appears to be a major controlling factor in the production of this feature. This process may be relevant for other case studies of carbonate platforms, as currents may be accelerated around such edifices, leading to slope winnowing and sediment deposition in more current-protected zones. The study results also have consequences for the interpretation of outcrop and seismic subsurface data of carbonate platform slope series, because such slope sediment wedges are not necessarily formed during sea-level highstands, but can consist of lowstand wedges only.

INTRODUCTION

When tropical carbonate platforms are flooded and the platform interior is occupied by a neritic carbonate factory, sediment is exported into the adjacent basins, especially towards the leeward flanks of the platform where this sediment is redistributed through wind-driven currents and waves (Eberli & Ginsburg, 1987). This process has been defined as highstand shedding (Schlager *et al.*, 1994), which is the main mechanism to form the slope sediments that accumulate into wedge-shaped bodies. Because the amount of sediment deposited during sea-level highstands is larger than the amount formed during sea-level lowstands (Grammer & Ginsburg, 1992), carbonate platform slope wedges mainly consist of highstand deposits. Intrinsic factors, such as an oversteepening of the slope or differences in the grain size of the exported particles, were evoked as controlling factors to allow slope sediment bypass or even erosion (Schlager & Camber, 1986; Kenter, 1990; Rendle-Bühring & Reijmer, 2005). This concept of a highstand origin for slope deposits is well established and applied when interpreting subsurface and outcrop data from carbonate platform slopes.

There is, however, growing evidence that gravitationally controlled off-bank transport mechanisms are only one factor controlling carbonate platform slope deposits and that alongslope contour currents are another major driver of slope deposition. This has been shown at the different slopes of the Bahamas carbonate platform, where the highstand sediments accumulate in periplatform drifts, i.e. drift bodies lining the platform flanks (Betzler *et al.*, 2015; Tournadour *et al.*, 2015; Chabaud *et al.*, 2016; Principaud *et al.*, 2016; Wunsch *et al.*, 2016), irrespective of the windward or leeward exposure of the slope. Slope segments with elevated contour current velocities show no sediment cover or reduced sedimentary thickness (Neumann & Ball, 1970; Mulder *et al.*, 2012).

The Maldives archipelago consists of atolls bathed by vigorously flowing and seasonally reversing currents (Betzler *et al.*, 2009, 2013a, 2016; Lüdmann *et al.*, 2013). Therefore, the atoll slopes appear to be a good location to study the interaction of currents and sea-level controlled slope sedimentation and to expand the insights into the interaction of carbonate slope sedimentation and contour currents. It will be shown that the established lowstand–highstand partition is not applicable because virtually no highstand material is deposited along the slope.

GEOLOGICAL SETTING

The Maldives archipelago south-west of India, in the central equatorial Indian Ocean, is an isolated tropical carbonate platform (Fig. 1). The north–south-oriented double row of atolls encloses the Inner Sea of the Maldives (Fig. 1A). Atolls are separated from each other by inter-atoll channels, which deepen towards the Indian Ocean (Purdy & Bertram, 1993). The Inner Sea is a bank-internal basin with water depths of up to 550 m (Fig. 1B). The Maldives carbonate sedimentary succession is almost 3 km thick and has accumulated since the Eocene, away from any terrigenous input (Aubert & Droxler, 1992; Purdy & Bertram, 1993; Belopolsky & Droxler, 2004; Betzler *et al.*, 2009, 2013b).

The archipelago comprises about 1200 smaller atolls. Discontinuous marginal rims formed by smaller atolls (faros) surround lagoons with water depths of up to 50 to 60 m (Betzler *et al.*, 2015). The oceanward margins of the Maldives archipelago are generally steeply inclined, with dips of 20 to 30° down to 2000 m of water depth. On the Inner Sea side, stepped atoll slopes have the same dip angles, but reach down to water depths of a few hundred metres, where the gradient rapidly declines (Fürstenau *et al.*, 2010). The Inner Sea is characterized by periplatform ooze deposition (Droxler *et al.*, 1990), locally accumulated into sediment drift bodies (Betzler *et al.*, 2009, 2013a,b; Lüdmann *et al.*, 2013).

The climate and oceanographic setting of the Maldives is dictated by the seasonally reversing Indian monsoon system (Tomczak & Godfrey, 2003). South-western winds prevail during the northern hemisphere summer (April to November), whereas northeastern winds prevail during winter (December to March). Winds generate ocean currents, which are directed westwards in the winter and eastwards in the summer. Interseasonally, a band of Indian Ocean Equatorial Westerlies establishes strong, eastward-flowing surface currents with velocities of up to 1·3 m s^{-1}. Currents reach down to the sea floor (Lüdmann *et al.*, 2013), especially in the inter-atoll passages, where submarine dunes and moats occur (Betzler *et al.*, 2009, 2013b).

METHODS

Seismic signals were generated by means of two clustered GI-Guns. The volume of each GI-Gun was 45 cin for the generator with a 105 cin injector volume. The GI-Guns were operated in 'true GI mode' and synchronized by a SureShot trigger system, which displays the source signal of each airgun. The digital streamer used for the survey was a Hydroscience Technologies SeaMUX 144-channel array with an active length of 600 m and an asymmetric group interval. The selected shooting distance during the entire cruise was 25 m.

Sub-bottom data were recorded with the RV METEOR parametric sediment echo sounder (PARASOUND P70; Atlas Elektronik, Bremen, Germany). The system was operated with two frequencies (18 kHz and 22 kHz). The software PS32segy (Hanno Keil, University of Bremen, Germany) was used to cut and convert the data. Data processing was performed with the software package ReflexW (Sandmeier Software, Karlsruhe, Germany), comprising automatic gain control (AGC) and along-profile amplitude normalization.

Sediment samples were acquired with a piston corer during Cruise M74/4 with RV METEOR and a videograb sampler during Cruise SO236 with RV SONNE. Components in the sediments were analysed quantitatively: Samples were wet-sieved and 200 components from the 500 to 1000 μm and the >1000 μm fraction were counted. The following components were differentiated: *Amphistegina*, *Homotrema*, *Operculina*, *Heterostegina*, *Gyrodinoides*, miliolids, other benthic foraminifers, planktonic foraminifers, bryozoans (encrusting, robust branching, vagrant), bivalves, gastropods, echinoderms, serpulids, crustaceans, bioclasts and lithoclasts. Especially bioclasts in some samples have a dark grey to black stain. Such components were counted separately. Tables with the counts are deposited at www.pangaea.de.

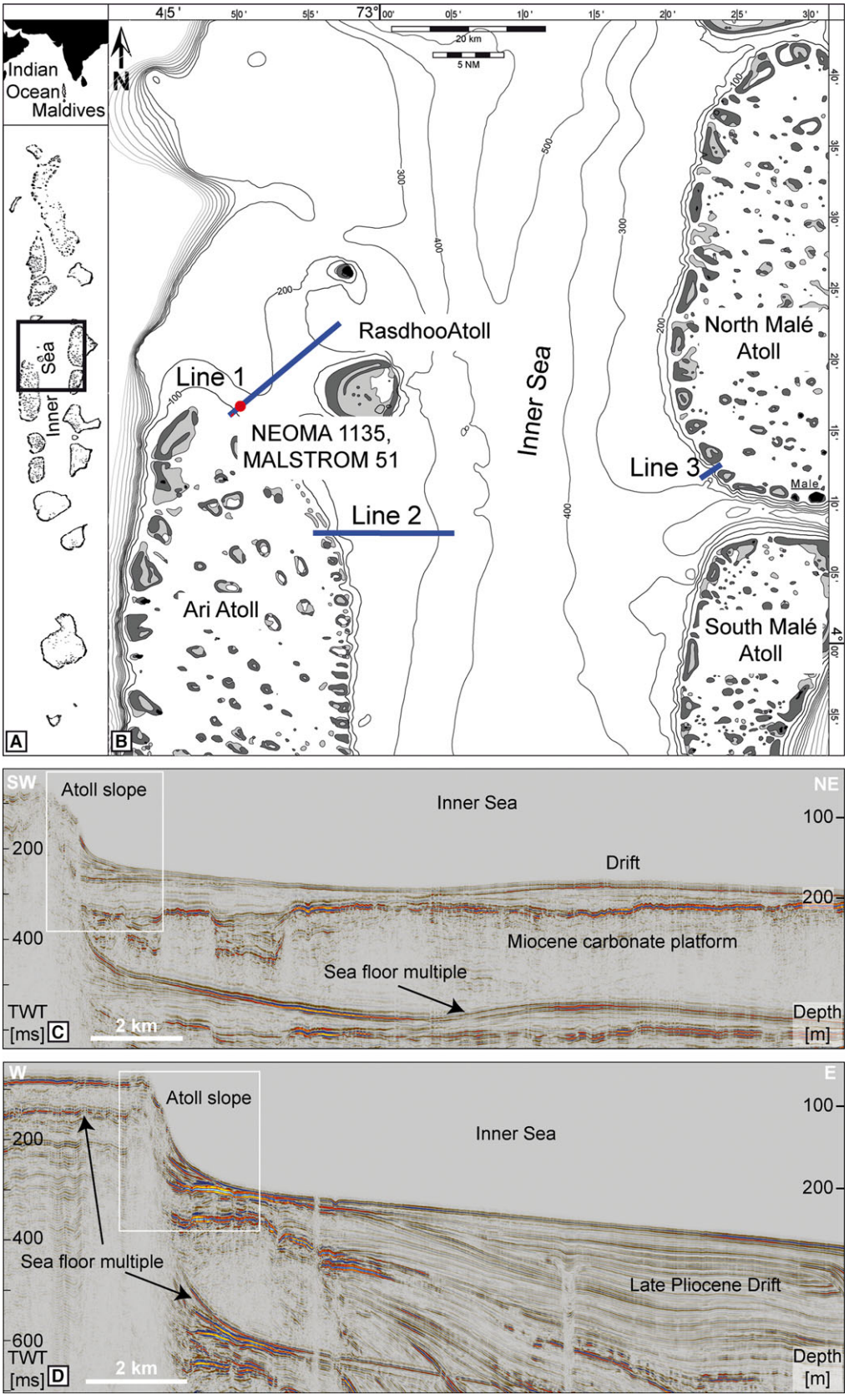

Fig. 1. (A) Double row of Maldives atolls enclosing the Inner Sea. The rectangle indicates location of B with seismic lines shown and discussed herein. (C) Overview seismic line from Ari Atoll into the Inner Sea. Note the basinward thinning of the stacked slope wedges. Rectangle indicates the position of the detailed view in Fig. 2A. (D) Overview seismic line from Ari Atoll into the Inner Sea. Note the basinward thinning of the stacked slope wedges and that the succession in the Inner Sea consists of drifts. Rectangle indicates the position of the detailed view in Fig. 2B. [Colour figure can be viewed at wileyonlinelibrary.com]

Radiocarbon dating was performed by Beta Analytics Inc. (Miami, FL, USA) on selected calcareous microfossils and macrofossils (Table 1). Samples were ultrasonically cleaned in deionized water and visually inspected for cements, overgrowths and fills. Conventional radiocarbon ages were calibrated using Calib (v.7.0.4, Stuiver & Reimer, 1993) and the calibration curve Marine13 (Reimer *et al.*, 2013) with no local reservoir correction applied. Calibrated ages were rounded to the next decade, and in the text, the median of the probability distribution is used in conjunction with the two-sigma range (95·4% probability).

RESULTS

Seismic data

During the M74/4 cruise, the rims of the Ari and Male atolls were crossed three times at different positions in passages separating the faros lining the atoll's borders (Fig. 1B); overview lines are presented in Fig. 1C and D. Both atolls are around 50 m deep, and the passages between the faros have a slightly shallower sill before the stepped slopes dip at 10 to 50° into the Inner Sea. The Inner Sea is between 200 and 430 m deep, with the deepest area in its central part. Whereas seismic imaging of the lagoonal stratigraphy is reduced because of the seafloor multiple, data from the slopes and the Inner Sea give a good insight into the stratigraphic succession (Figs 1C, D, and 2). The Inner Sea succession consists of a drowned carbonate bank lined and overlain by drift deposits (Fig. 1C), similar to the succession of the Kardiva Channel located further north in the Maldives archipelago (Betzler *et al.*, 2009, 2013a, 2016; Lüdmann *et al.*, 2013).

Line 1, located at the northeastern margin of Ari Atoll is oriented NE-SW and crosses the position of Core M74/4-1135 and of videograb sample SO236-51 (Figs 1B, C and 2A). Down to a water depth of 100 m, the line images an irregular sea-floor relief on top of a succession with discontinuous to chaotic reflections. From *ca* 97 to 128 m, there is a submarine cliff. Basinwards, the slope progressively flattens out to water depths of 180 m. Here, reflections are laterally more or less continuous with moderate amplitudes. Strong, slightly inclined reflections occur in the upper part of the succession, which appear truncated downslope. Around 8 km NE of the platform edge, the deposits are arranged into drift bodies (Fig. 1C).

Line 2 (Figs 1B, D and 2B) is located at the eastern margin of Ari Atoll. Similar to the northeastern margin of the atoll (Line 1), there is a sea-floor step at *ca* 97 m. In front of this step, there is a sediment wedge with strong basinward reflections, which are also truncated downslope. This wedge overlies a horizon with a strong acoustic impedance, which corresponds to the limit between the Inner Sea drift units 8 and 9 (Lüdmann *et al.*, 2013), which was formed at *ca* 2·3 Ma (Betzler *et al.*, 2016). Drifts sediments form the succession further away from the atoll margin (Fig. 1D).

A sediment wedge is also imaged in Line 3 (Figs 1B and 2C), which crosses the south-western margin of North Malé Atoll. Towards the Inner Sea, the smooth pattern of reflection changes into a discontinuous to wavy

Table 1. Results of radiocarbon dating. Calibration was performed using Calib (v7.0.4, Stuiver & Reimer, 1993) and the calibration curve Marine13 (Reimer *et al.*, 2013). No local reservoir correction was applied

	Depth			^{14}C age	^{13}C/^{12}C ratio	Calibrated age (ΔR = 0)	
						cal BP (2σ ranges, 95·4% prob.)	
	mbsf	Lab ID	Material	yrs BP	‰	Range (years)	Median (ka)
Core 1135	0·66	Beta-271838	Bivalve	13 800 ± 60	+1·1	15 900 to 16 310	16·12 ± 0·21
Core 1135	3·66	Beta-265298	Coral	14 400 ± 70	−2·0	16 670 to 17 260	16·99 ± 0·30
Core 1135	5·66	Beta-265299	Coral	15 230 ± 70	−2·5	17 840 to 18 250	18·03 ± 0·21
Core 1135	6·99	Beta-265297	Bivalve	15 490 ± 70	+1·5	18 100 to 18 540	18·33 ± 0·22
Core 1135	9·16	Beta-271839	Bivalve	18 740 ± 70	−1·0	21 950 to 22 410	22·22 ± 0·23
SO236-51	0	Beta-432465	*Amphistegina*	11 850 ± 40	−0·6	13 210 to 13 430	13·32 ± 0·11

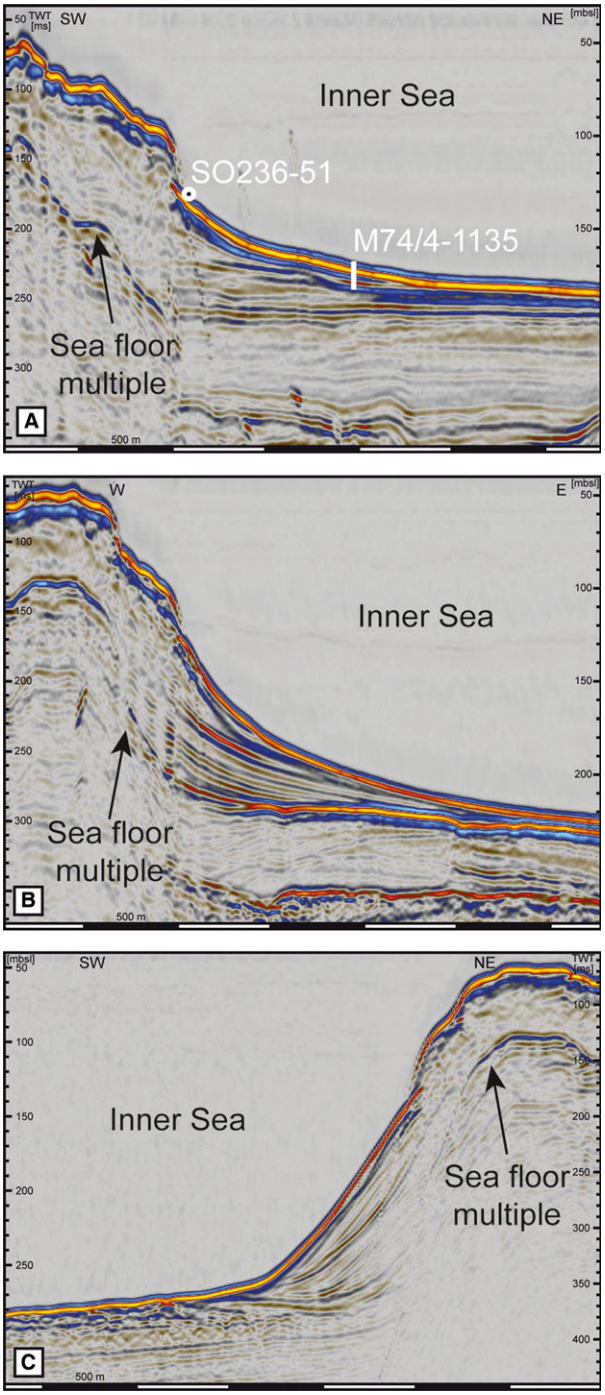

Fig. 2. (A) Seismic line 1 from the Inner Sea across the flank of Ari Atoll with location of piston core M74/4-1135 and videograb sample SO236-51 (B). (C) Seismic line 2 from the Inner Sea across the flank of Ari Atoll (D). (E) Seismic line 1 from the Inner Sea across the flank of North Malé Atoll (B). Vertical exaggeration: A – D = 10 X, F, F = 8 X. [Colour figure can be viewed at wileyonlinelibrary.com]

stratification which corresponds to an area where the sea floor is covered by submarine dunes moved by bottom currents (Betzler *et al.*, 2013a; Lüdmann *et al.*, 2013).

Sedimentology

Piston Core M74/4-1135 was retrieved at 4°16′59·592″N, 72°50′4·992″E, i.e. around 2 km NE of the margin of Ari Atoll at a water depth of 172 m (Figs 2A and 3A, B). It recovered 12·22 m of unlithified carbonates with a rudstone to grainstone texture (Fig. 4) deposited in the sediment wedge located in front of the 30 m high submarine cliff which forms the seaward limit of the terrace at a water depth of *ca* 97 m.

Figure 3 depicts the linkage between sedimentological and high-resolution parasound data. The parasound profile images a surface with a high impedance contrast at a depth of 7 mbsf (metre below sea floor). In the core, this surface correlates with a colour change from dark greenish grey to grey. The darker core colours are due to the high abundance of dark components giving the sediment a 'salt-and-pepper' texture (Fig. 5A). The dark colour of the grains is a consequence of an elevated organic and clay content, as resolved in smear slides of acid residues.

The lower 30 cm of the succession consists of a rhodolith-rich rudstone with a fining-upward trend of the components. Between 11·92 mbsf and 8·80 mbsf, the core is a grey rudstone with some dispersed rhodoliths up to 5 cm in size. Above 8·8 mbsf, a rudstone with some rhodoliths is mottled with a greenish grey to grey colour. A platy coral was recovered at 6·7 mbsf. Large components disappear upcore, with the last large rhodoliths registered at 5·5 mbsf. The top of the succession is a light grey packstone to grainstone with *Halimeda* flakes, planktic foraminifers, pteropods, benthic foraminifers, serpulids and echinoid debris (Fig. 5B).

Out of the differentiated and counted components in the fraction >1 mm, some show distinct trends with depth. The variation in abundance of these components is presented in Fig. 4. From the bottom of the core, *Amphistegina* and *Operculina* decrease in abundance upcore from around 15% and 25% of the components, respectively, to almost disappearing in the upper part of the sequence. Red algae and the green alga *Halimeda* show an inverse trend increasing upcore to reach 10% to 15% and 40% of the particles, respectively. Bioclasts decrease in abundance upcore, as is the case for the stained dark bioclasts, which make up 40% to 45% of the samples below 9·6 mbsf. In contrast to the trend described for the other components which extend over

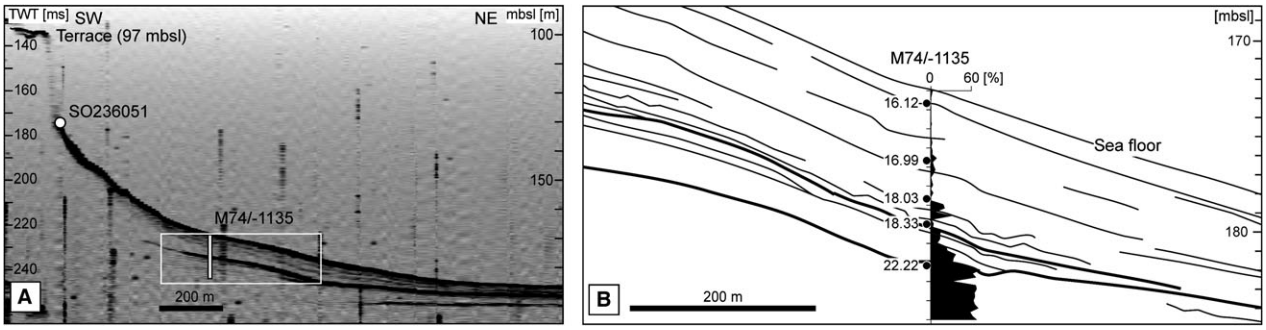

Fig. 3. (A) Parasound line covering the submarine terrace, the submarine cliff and the sediment wedge on the northern flank of Ari Atoll. (B) Detail view of the same parasound line showing the succession around Site M74/4-1135. The abundance of the dark grains (see also Fig. 4) is shown on the curve as an orientation to allow comparison of variations in abundance of components (Fig. 4) with the physical stratigraphy. [Colour figure can be viewed at wileyonlinelibrary.com]

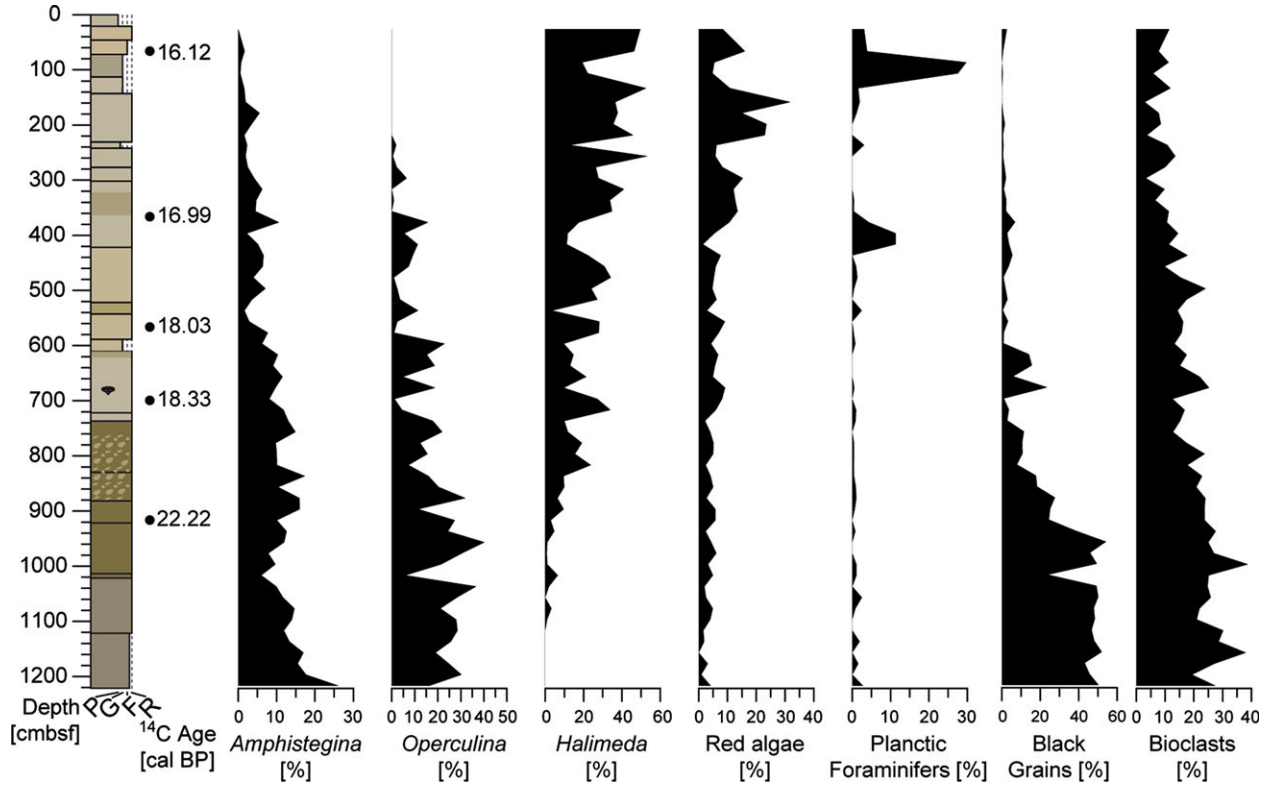

Fig. 4. Lithological column of core M74/4-1135 with variations in the relative abundance of selected components and position of samples used for radiocarbon dating. [Colour figure can be viewed at wileyonlinelibrary.com]

the entire core, the abundance of the dark bioclasts rapidly decreases between 9·6 mbsf and 7·4 mbsf to values of 0% to 5% above, except for the interval between 6·8 mbsf and 6·2 mbsf, where 10% to 20% were counted.

Red algae from selected rhodolith samples (Table 2) were analysed in thin section for identification at the most precise taxonomic level possible. Among coralline red algae, the dominating genus is *Lithothamnion*, followed by *Lithophyllum* and minor *Lithoporella*. The aragonitic red alga *Peyssonnelia* occurs in several samples as well.

Five samples were used for age dating the succession (Fig. 4, Table 1) suggesting that the interval between 0·66 mbsf and 9·16 mbsf was deposited between

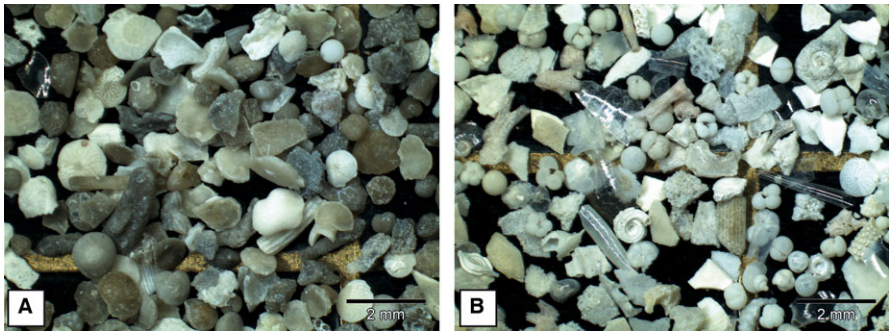

Fig. 5. Microphotograph of components >500 μm at Site M74/4-1135. (A) Sample from a core depth of 11·95 mbsf with abundant darkened bioclasts, *Amphistegina*, *Operculina*, red algal debris and minor planktic foraminifers. (B) Sample from a core depth of 0·65 mbsf with planktic foraminifers, pteropods, serpulids, echinoid debris and benthic foraminifers. [Colour figure can be viewed at wileyonlinelibrary.com]

Table 2. Red algae in selected samples of Core M74/4-1135. The samples in grey include components common in the 'intermediate water assemblage' of Webster *et al.* (2009), namely *Lithophyllum acrocamptum* and *Lithothamnion prolifer*

Sample	Depth (mbsf)	Algae
1135-2-5H-90-100	5·16	*Lithothamnion prolifer, Lithophyllum acrocamptum, Hydrolithon* sp., *Lithophyllum* gr. *pustulatum*, *Mesophyllum* sp.
1135-2-6G-30-35.1	5·56	Laminar *Lithothamnion, Lithoporella* sp., *Lithophyllum acrocamptum*?
1135-2-6G-30-35.2	5·56	Laminar *Lithothamnion*, *Lithoporella* sp., *Peyssonnelia* sp.
1135-2-7D-60-65	6·86	Laminar *Lithothamnion*, *Lithophyllum* gr. *pustulatum*, *Peyssonnelia* sp.
1135-2-9D-10-15	8·36	Laminar *Lithothamnion*, *Spongites*? sp., *Peyssonnelia* sp.
1135-2-9D-80-87	9·06	Laminar *Lithothamnion*, *Lithophyllum* gr. *pustulatum*, *Peyssonnelia* sp.
1135-2-10C-55-57.1	9·76	*Lithothamnion prolifer* (heavily bored) in the nucleus, laminar *Lithothamnion*, *Peyssonnelia* sp.
1135-2-10C-55-57.2	9·76	Laminar *Lithothamnion*, *Lithophyllum* gr. *pustulatum*, *Peyssonnelia* sp.
1135-2-10C-95-100	10·16	Laminar *Lithothamnion*, *Peyssonnelia* sp.
1135-2-12A-22	11·44	Laminar *Lithothamnion*, *Lithophyllum acrocamptum*, *Lithoporella* sp.
1135-2-12A-94-100	12·16	Laminar *Lithothamnion*, *Lithophyllum acrocamptum*?, *Lithoporella* sp.

approximately 16 and 22 ka BP. Deposits below 9·16 mbsf were not dated, as fossils without encrustation were not found. Three intervals with distinct sedimentation rates can be differentiated: below 7 mbsf, the rate is around 0·6 mm year^{-1}, between 7 and 0·66 mbsf the values increase to 3·9 mm year^{-1} before dropping sharply to 0·04 mm year^{-1}.

Videograb sample SO236-51 is located at the toe of a 31 m high terrace which is positioned at a water depth of *ca* 97 m (Fig. 3A). The 132 m deep location is 500 m upslope of Site M74/4-1135. The sea floor at the sample locality and along the flank of Ari Atoll is an irregular rocky surface (Fig. 6A and B). The rock is a rudstone (Fig. 6C) with large benthic foraminifers (*Amphistegina*, *Heterostegina*, *Alveolinella*), encrusting and articulated red algae, encrusting foraminifers and bryozoa, *Halimeda* flakes, serpulids and planktonic foraminifers. The irregular rock surface, colonized by gorgonians, sponges and bryozoa, is characterized by holes and depressions with irregular shapes (Fig. 6B). For age dating of these deposits, several *Amphistegina* specimens were isolated which yield an age of around 13·32 ± 0·11 ka cal BP.

INTERPRETATION AND DISCUSSION

Depositional geometry

The three seismic lines depicted in Fig. 2 cover the transition from the reef buildups of the atoll margins to the stratified succession of the fore-reef area and the basin. This transition is characterized by a change from discontinuous and chaotic reflections to more continuous reflections from the sediment wedges. The limit between both acoustic facies is placed at the toe of the 31 m high wall of the 97 m terrace, which has been attributed to reefs which drowned during Meltwater Pulse 1A (14·3 to 14·65 kyrs BP; Deschamps *et al.*, 2012) by Fürstenau *et al.* (2010). The successions of the different slopes analysed are arranged into an aggrading to slightly backstepping pattern (Fig. 2).

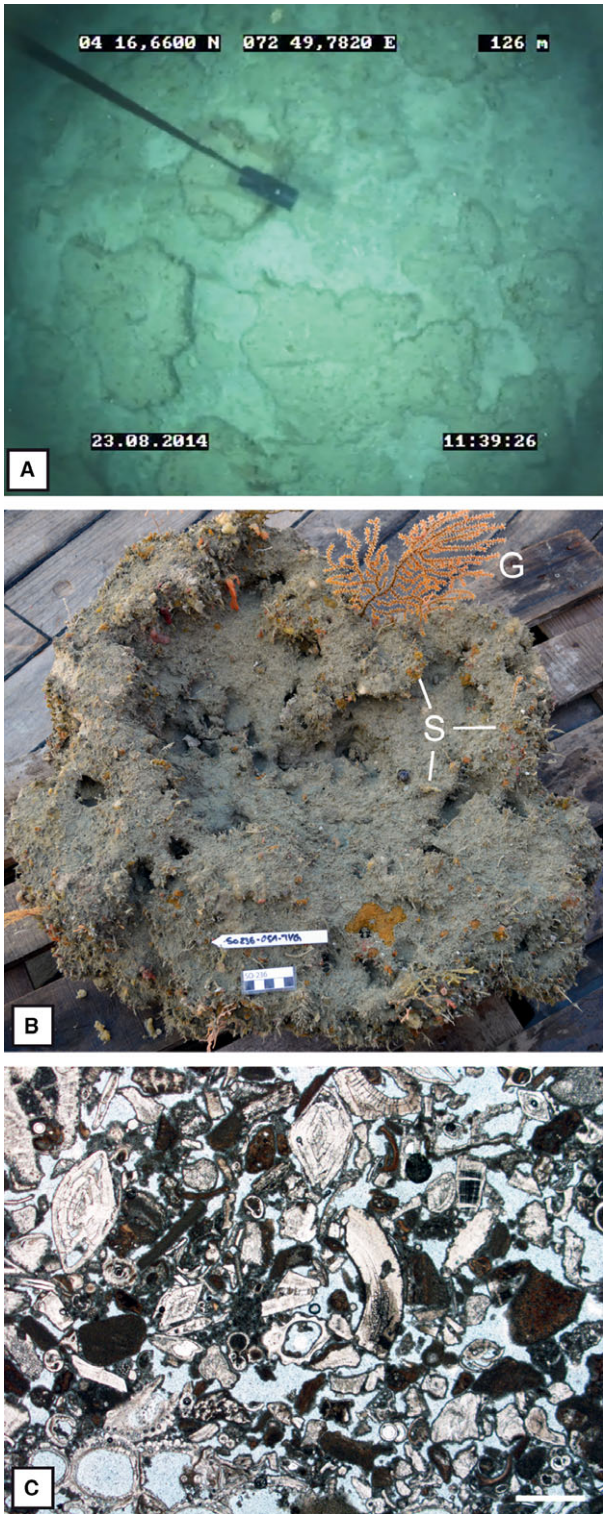

Fig. 6. (A) Underwater photograph of the irregular and rocky sea floor in the vicinity of the location of sample SO236-051. Numbers at the top of the photograph display the geographical location and the water depth. (B) Videograb sample SO236-051 on deck of RV SONNE just after recovery. The irregular block is overgrown by gorgonians (G), sponges (S) and bryozoa. Scale: 5 cm. (C) Thin section photograph of Videograb sample SO236-051 with a high interparticle porosity, abundant *Amphistegina*, bryozoa, planktic foraminifers, *Halimeda* debris and bioclasts. Scale bar: 0·5 mm. [Colour figure can be viewed at wileyonlinelibrary.com]

Lowstand sediment wedges

The sediment wedges were formed during the last glacial sea-level lowstand, as indicated by the dating of the core M74/4-1135, which shows that the succession was deposited between *ca* 22 and 16 kyrs BP (Table 1, Fig. 7). Applying the reconstruction for the sea-level position during and after the last glacial maximum (Deschamps *et al.*, 2012; Lambeck *et al.*, 2014), the site would have been located at water depths of *ca* 48 m at 22 kyrs BP, *ca* 55 m at 18 kyrs BP, *ca* 52 m at 16·9 kyrs BP and *ca* 57 m at 16 kyrs BP (Figs 7 and 8).

In general, Core M74/4 displays an upcore trend from a floatstone to rudstone to a packstone to grainstone texture. The red algal associations and the large benthic foraminifers provide two lines of evidence indicating that the deposits recovered in Core M74/4-1135 were formed *in situ* within this palaeobathymetric range, or are parautochthonous at most. The samples marked by grey shading in the red algal overview of Table 2 include components common in the 'intermediate water assemblage' of Webster *et al.* (2009), namely *Lithophyllum* gr. *acrocamptum* and *Lithothamnion prolifer*. In the Pacific Ocean, in the absence of shallow-water species, such as *Porolithon onkodes*, these coralline algae are typical of 20 to 60 m water depths; a similar depth range, however, can be expected for the Indian Ocean, where less data are available. This covers the water depth of *ca* 50 m for the site location applying the Deschamps *et al.* (2012) sea-level curve. In any case, this depth range obviously can change in extremely clear waters, which however, in the discussed case study is irrelevant, as the maximum water depth at the time of sedimentation is constrained by the sea-level position (Fig. 8).

The large benthic foraminifer *Operculina ammonoides*, which is frequent to abundant in the lower and middle part of the succession (Figs 4 and 7), lives in water depths of up to 70 m with an optimum around 40 m (Hohenegger, 2000). *Amphistegina lessoni* and *A. radiata* are also frequent to abundant and thrive in water depths of up to 70 m, with highest abundance around 40 m (Hohenegger, 2000). As is the case for the red algae, the palaeobathymetry indicated by the large benthic foraminifers in the succession falls within the water depth for the site (Deschamps *et al.*, 2012). Both large benthic foraminifer decrease in abundance as the water depth at Site M74/4-1135 deepened (Fig. 7). This trend is paralleled by

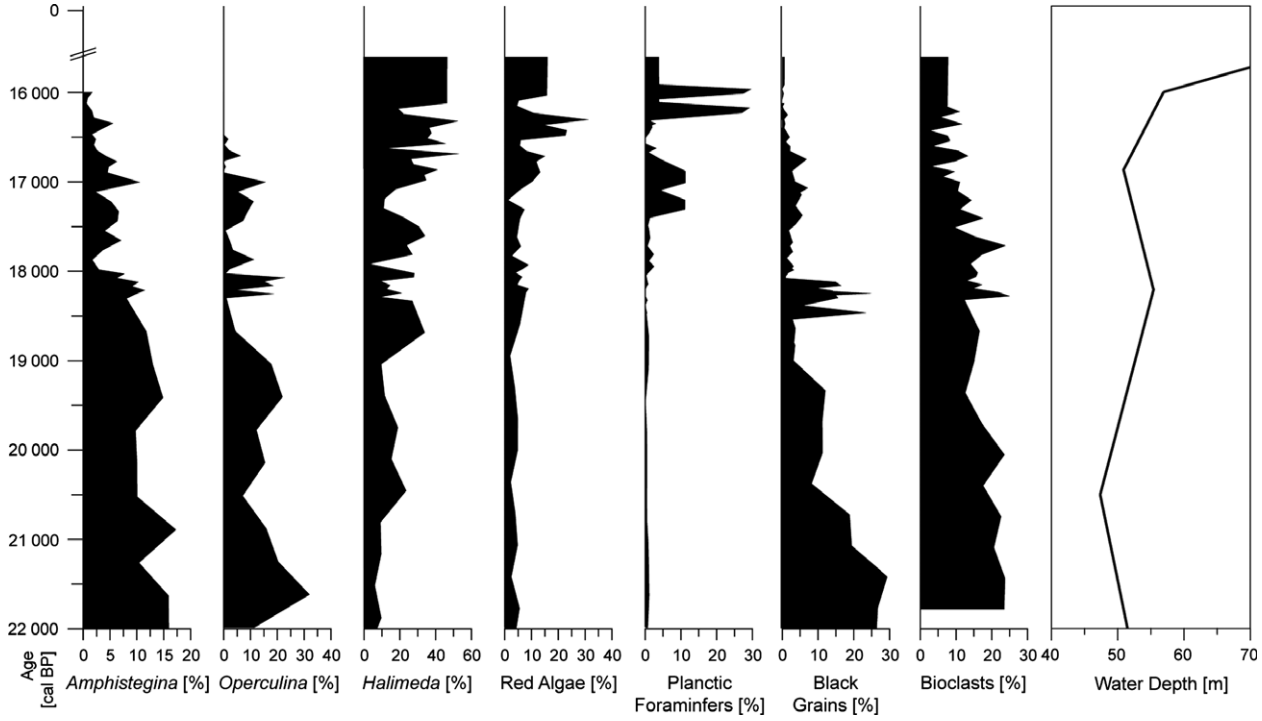

Fig. 7. Compositional variation of selected components in Core M74/4-1135 against age (position of samples used for age model is shown in Fig. 4). In the right-hand side of the figure, the variations in water depth at Site M74/4-1135 are shown, using the sea-level curve by Deschamps *et al.* (2012) and Lambeck *et al.* (2014).

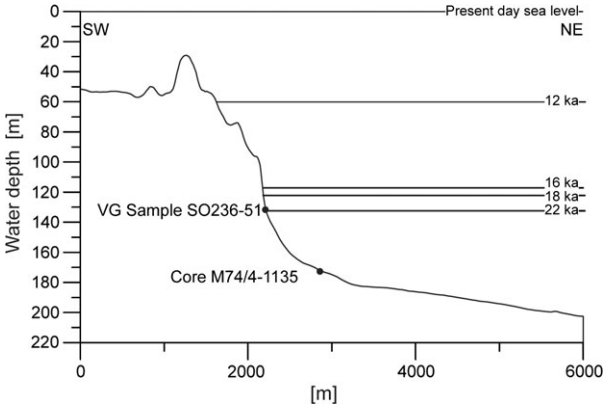

Fig. 8. SW–NE section through the northern flank of Ari Atoll along the position of seismic line 1 (see Fig. 1B for location) with sea-level stands between 22 ky BP and today.

increased amounts of *Halimeda* and red algae. In the Indo-Pacific, *Halimeda* and red algae may be more abundant at water depths exceeding those occupied by large benthic foraminifers (Wilson & Vecsei, 2005). Therefore, the upcore increase in algal abundance may well be a consequence of the deepening of Site M74/4-1135 during the post-glacial sea-level rise.

The dark-stained grains (Fig. 4) record a certain sediment influx from the exposed carbonate platform. In carbonates, such grains blackened by organics and clays are known from intertidal and subtidal environments (Flügel, 2004). It is proposed that in Core M74/4-1135, these grains were shed from the emerging parts of the platform, which were just some hundreds of metres away from the site location. This export was reduced with the transgression due to the beginning of sea-level rise around 20·5 ka BP (Lambeck *et al.*, 2014) to recover a little bit around 18·5 ka BP with the temporary stop of sea-level rise at that time (Fig. 7). The base of this transgression correlates with the high-amplitude reflection in the parasound profile which crosses the core location (Fig. 3).

In summary, data indicate that the sediment wedge at position of Site M74/4-1135 is a lowstand wedge and that no or only very minor sediment is deposited in this area during the latest Pleistocene and Holocene. The parallelism in shape and seismic stratigraphy of this wedge compared with the other wedges as imaged in the seismic lines (Fig. 2) indicate that this also applies to other atoll flanks.

Intrinsic and extrinsic control on slope deposition

The seminal publication by Schlager *et al.* (1994) established the concept of the highstand shedding of Quaternary tropical flat-topped carbonate platforms, where the

platforms export sediment into the adjacent basins when they are flooded and a shallow-water carbonate factory produces particles. Limitations were seen for carbonate ramps and carbonate platforms undergoing sea-level lowstands for extended periods of time. Applying the highstand shedding scenario, carbonate platform slope angles are seen as a function of grain size (Kenter, 1990), with coarser-grained sediments developing steeper slope angles than finer-grained ones. Both aspects are now widely accepted paradigms of carbonate sedimentology and stratigraphy applied when interpreting geological and subsurface geophysical data.

In the carbonate sedimentary succession of the Maldives, a differentiation of highstand and lowstand deposition has been demonstrated for the Pleistocene and Holocene drifts of the Inner Sea by Paul *et al.* (2012) and Betzler *et al.* (2013b). This is based on variations in the amount of fine-grained, platform-derived aragonite mud which at different basinal localities of the Maldives is most abundant in the highstand deposits. Therefore, it remains to be resolved why the slope and toe of slope deposits do not bear highstand sediments.

Sediment export by highstand shedding does not necessarily imply deposition at the slope of the carbonate platform, because other processes may outweigh gravitational transport processes. In carbonates, slope steepening behind the angle of repose has been suggested as an intrinsic mechanism allowing slope bypass of sediment exported from the platform into the basin (Schlager & Camber, 1986). The Bahamas escarpment has been reported as the type example to illustrate the case of slope sediment bypass. This, however, has to be revised because a number of recent studies show that along-slope contour currents winnow the slope and toe of slope (Mulder *et al.*, 2012; Betzler *et al.*, 2015; Jo *et al.*, 2015; Lüdmann *et al.*, 2016; Principaud *et al.*, 2016; Wunsch *et al.*, 2016). Consequently, it is reworked deposits that accumulate in periplatform drifts (Betzler *et al.*, 2015) and in detached drifts in the basin (Bergman *et al.*, 2010; Lüdmann *et al.*, 2016).

Large drifts in the Inner Sea together with submarine dunes show that currents also dictate sedimentation patterns in the Maldives (Fig. 1C and D) (Betzler *et al.*, 2009, 2013a,b, 2016; Lüdmann *et al.*, 2013). Current speeds in the channels between the atolls are typically in the range of 0·5 to 0·8 m s^{-1} and accelerate in the interfaro channels and along the atoll flanks to 1·5 to 2·6 m s^{-1} (Preu & Engelbrecht, 1991; Owen *et al.*, 2011). These currents are the result of the interaction of ocean, tidal and wind-induced currents. As noted by Darwin (1842, p. 108), based on the reports of Capt. Moresby, 'The currents of the sea flow across these atolls (…) yet the currents sweep with greater force round their flanks'. The effect of these currents is well-documented in the video survey performed along the flank of Ari Atoll around the location of Sample SO236-51, where the sea floor is rocky, with no sediment cover (Fig. 6A). A question which remains unanswered based on available data is if the current regime flowing around the atolls was different during the past sea-level lowstand thus allowing lowstand deposition.

The margin aggradation or backstepping (Fig. 2) in the Maldives can be traced back to the lower Pliocene (Betzler *et al.*, 2013a). Such a pattern elsewhere is interpreted to reflect carbonate platform growth under increasing accommodation, but the long-term platform trend discards sea-level changes as a trigger as it also applies to the rate of subsidence which has been calculated to be around 0·03 to 0·04 mm $year^{-1}$ over the long term (Belopolsky & Droxler, 2004) and to 0·15 mm $year^{-1}$ for the short term (Gischler *et al.*, 2008). The onset of the growth pattern correlates rather with the early Pliocene widening of the inter-atoll passages as mapped by Lüdmann *et al.* (2013). Inner Sea drift geometries indicate that the opening and widening of the passages allowed the current system that controls sedimentation nowadays to be established.

Summarizing, it is proposed that alongslope currents redistribute the sediment formed during the highstand shedding away from the atoll slopes, where the highest current speeds are to be expected, towards the more protected and tranquil areas of the Inner Sea. These are the zones of the Inner Sea, where large drift bodies accumulate (Fig. 1C and D). These drift sediments show a clear differentiation into aragonite-mud rich highstand deposits and aragonite poor lowstand deposits (Paul *et al.*, 2012; Betzler *et al.*, 2013b). Self-erosion of the slope (Schlager & Camber, 1986) is excluded because the seismics and parasound lines do not show the corresponding signatures (Fig. 2).

CONCLUSIONS

The slope successions of atolls in the Maldives archipelago consist of a series of basinward thinning wedges which were deposited during sea-level lowstands, whereas highstand deposits are condensed. Rather than intrinsic factors such as slope steepness, the vigorous currents around and in the atolls control this pattern. Highstand sediment is not accumulated along the slope but reworked and transported to be accumulated into drift deposits forming in current-protected areas. This observation confirms that contour currents are of equal importance for determining carbonate sedimentation patterns on carbonate platform slopes as is, for example, the windward–leeward orientation of the slope. This effect of contour currents is expected to be more

common in the geological record of carbonate platform slopes than previously estimated.

ACKNOWLEDGEMENTS

The authors thank the officers and the crew of the RV METEOR during Cruise M74/4 and of RV SONNE during Cruise SO236 MALSTROM for their efficient assistance and the Shipboard Scientific Parties for the substantial support. Jörn Fürstenau and Hauke Petersen are thanked for their contributions within the project NEOMA. The German Federal Ministry of Education and Research is thanked for funding (03S0405, 03G0236A), the Ministry of Fisheries and Agriculture of the Maldives for granting the research permit for Maldivian waters. Thanks to the editor P. Swart and associate editor A. Klaus for their editorial support.

CONFLICT OF INTEREST

The authors declare that they have no conflict of interest.

References

Aubert, O. and **Droxler, A.W.** (1992) General Cenozoic evolution of the Maldives carbonate system (equatorial Indian Ocean). *Bull. Centres Rech. Explor.-Prod. Elf-Aquitaine*, **16**, 113–136.

Belopolsky, A.V. and **Droxler, A.W.** (2004) Seismic expressions and interpretations of carbonate sequences: the Maldives carbonate platform, equatorial Indian Ocean. *AAPG Stud. Geol.*, **49**, 57.

Bergman, K.L., Westphal, H., Janson, X., Poiriez, A. and **Eberli, G.P.** (2010) Controlling Parameters on Facies Geometries of the Bahamas, an Isolated Carbonate Platform Environment. In: *Carbonate Depositional Systems: Assessing Dimensions and Controlling Parameters* (Eds H. Westphal, B. Riegl and G.P. Eberli), pp. 5–80. Springer, Heidelberg.

Betzler, C., Hübscher, C., Lindhorst, S., Reijmer, J.J.G., Römer, M., Droxler, A.W., Fürstenau, J. and **Lüdmann, T.** (2009) Monsoonal-induced partial carbonate platform drowning (Maldives, Indian Ocean). *Geology*, **37**, 867–870.

Betzler, C., Fürstenau, J., Lüdmann, T., Hübscher, C., Lindhorst, S., Paul, A., Reijmer, J.J.G. and **Droxler, A.W.** (2013a) Sea-level and ocean-current control on carbonate-platform growth, Maldives, Indian Ocean. *Basin Res.*, **25**, 172–196.

Betzler, C., Lüdmann, T., Hübscher, C. and **Fürstenau, J.** (2013b) Current and sea-level signals in periplatform ooze (Neogene, Maldives, Indian Ocean). *Sed. Geol.*, **290**, 126–137.

Betzler, C., Lindhorst, S., Lüdmann, T., Weiss, B., Wunsch, M. and **Braga, J.C.** (2015) The leaking bucket of a Maldives atoll: implications for the understanding of carbonate platform drowning. *Mar. Geol.*, **366**, 16–33.

Betzler, C., Eberli, G.P., Kroon, D., Wright, J.D., Swart, P.K., Nath, B.N., Alvarez-Zarikian, C.A., Alonso-García, M., Bialik, O.M., Blättler, C.L., Guo, J.A., Haffen, S., Horozal, S., Inoue, M., Jovane, L., Lanci, L., Laya, J.C., Mee, A.L.H., Lüdmann, T., Nakakuni, M., Niino, K., Petruny, L.M., Pratiwi, S.D., Reijmer, J.J.G., Reolid, J., Slagle, A.L., Sloss, C.R., Su, X., Yao, Z. and **Young, J.R.** (2016) The abrupt onset of the modern South Asian Monsoon winds. *Sci. Rep.*, **6**, 29838.

Chabaud, L., Ducassou, E., Tournadour, E., Mulder, T., Reijmer, J.J.G., Conesa, G., Giraudeau, J., Hanquiez, V., Borgomano, J. and **Ross, L.** (2016) Sedimentary processes determining the modern carbonate periplatform drift of Little Bahama Bank. *Mar. Geol.*, **378**, 213–229.

Darwin, C. (1842) *Structure and Distribution of Coral Reefs*. Smith, Elder & Co., London, 214 pp.

Deschamps, P., Durand, N., Bard, E., Hamelin, B., Camoin, G., Thomas, A.L., Henderson, G.M., Okuno, J.I. and **Yokoyama, Y.** (2012) Ice-sheet collapse and sea-level rise at the Bolling warming 14,600 years ago. *Nature*, **483**, 559–564.

Droxler, A.W., Haddad, G.A., Mucciarone, D.A. and **Cullen, J.L.** (1990) Pliocene-Pleistocene aragonite cyclic variations in Holes 714A and 716B (the Maldives) compared with Hole 633A (the Bahamas): records of climate-induced CaCO3 preservation at intermediate water depths. *Proc. ODP Sci. Results*, **115**, 539–577.

Eberli, G.P. and **Ginsburg, R.N.** (1987) Segmentation and coalescence of Cenozoic carbonate platforms, northwestern Great Bahama Bank. *Geology*, **15**, 75–79.

Flügel, E. (2004) *Microfacies of Carbonate Rocks*. Springer-Verlag, Berlin, 976 pp.

Fürstenau, J., Lindhorst, S., Betzler, C. and **Hübscher, C.** (2010) Submerged reef terraces of the Maldives (Indian Ocean). *Geo-Marine Lett.*, **30**, 511–515.

Gischler, E., Hudson, J.D. and **Pisera, A.** (2008) Late Quaternary reef growth and sea level in the Maldives (Indian Ocean). *Mar. Geol.*, **250**, 104–113.

Grammer, G.M. and **Ginsburg, R.N.** (1992) Highstand versus lowstand deposition on carbonate platform margins: insight from Quaternary foreslopes in the Bahamas. *Mar. Geol.*, **103**, 125–136.

Hohenegger, J. (2000) Coenoclines of larger foraminifera. *Micropaleontology*, **46**, 127–151.

Jo, A., Eberli, G.P. and **Grasmueck, M.** (2015) Margin collapse and slope failure along southwestern Great Bahama Bank. *Sed. Geol.*, **317**, 43–52.

Kenter, J.A.M. (1990) Carbonate platform flanks: slope angle and sediment fabric. *Sedimentology*, **37**, 777–794.

Lambeck, K., Rouby, H., Purcell, A., Sun, Y. and **Sambridge, M.** (2014) Sea level and global ice volumes from the Last Glacial Maximum to the Holocene. *Proc. Natl Acad. Sci. USA*, **111**, 15296–15303.

Lüdmann, T., Kalvelage, C., Betzler, C., Fürstenau, J. and **Hübscher, C.** (2013) The Maldives, a giant isolated carbonate platform dominated by bottom currents. *Mar. Pet. Geol.*, **43**, 326–340.

Lüdmann, T., Paulat, M., Betzler, C., Möbius, J., Lindhorst, S., Wunsch, M. and **Eberli, G.P.** (2016) Carbonate mounds in the Santaren Channel, Bahamas: a current-dominated periplatform depositional regime. *Mar. Geol.*, **376**, 69–85.

Mulder, T., Ducassou, E., Eberli, G.P., Hanquiez, V., Gonthier, E., Kindler, P., Principaud, M., Fournier, F., Léonide, P., Billeaud, I., Marsset, B., Reijmer, J.J.G., Bondu, C., Joussiaume, R. and **Pakiades, M.** (2012) New insights into the morphology and sedimentary processes along the western slope of Great Bahama Bank. *Geology*, **40**, 603–606.

Neumann, A.C. and **Ball, M.M.** (1970) Submersible observations in the Straits of Florida: geology and bottom currents. *Geol. Soc. Am. Bull.*, **81**, 2861–2874.

Owen, A., Kruijsen, J., Turner, N. and **Wright, K.** (2011) *Marine Energy in the Maldives*. Prefeasibility report on Scottish Support for Maldives Marine Energy Implementation, Main Report. Centre for Understanding Sustainable Practice, Robert Gordon University, Aberdeen, UK.

Paul, A., Reijmer, J.J.G., Fürstenau, J., Kinkel, H. and **Betzler, C.** (2012) Relationship between Late Pleistocene sea-level variations, carbonate platform morphology and aragonite production (Maldives, Indian Ocean). *Sedimentology*, **59**, 1540–1658.

Preu, C. and **Engelbrecht, C.** (1991) Patterns and processes shaping the present morphodynamics of coral reef islands. Case study from the North-Male atoll, Maldives (Indian Ocean). In: *From the North Sea to the Indian Ocean* (Eds H. Brückner and U. Radtke), pp. 209–220. Franz Steiner, Stuttgart.

Principaud, M., Ponte, J.P., Mulder, T., Gillet, H., Robin, C. and **Borgomano, J.** (2016) Slope-to-basin stratigraphic evolution of the northwestern Great Bahama Bank (Bahamas) during the Neogene to Quaternary: interactions between downslope and bottom currents deposits. *Basin Res.*. doi:10.1111/bre.12195.

Purdy, E.G. and **Bertram, G.T.** (1993) Carbonate concepts from the Maldives, Indian Ocean. *AAPG Stud. Geol.*, **34**, 56.

Reimer, P.J., Bard, E., Bayliss, A., Beck, J.W., Blackwell, P.G., Ramsey, C.B., Buck, C.E., Cheng, H., Edwards, R.L., Friedrich, M., Grootes, P.M., Guilderson, T.P., Haflidason, H., Hajdas, I., Hatté, C., Heaton, T.J., Hoffmann, D.L., Hogg, A.G., Hughen, K.A., Kaiser, K.F., Kromer, B., Manning, S.W., Niu, M., Reimer, R.W., Richards, D.A., Scott, E.M., Southon, J.R., Staff, R.A., Turney, C.S.M. and **van der Plicht, J.** (2013) IntCal13 and MARINE13 radiocarbon age calibration curves 0-50000 years cal BP. *Radiocarbon*, **55**, 1869–1887.

Rendle-Bühring, R.H. and **Reijmer, J.J.G.** (2005) Controls on grain-size patterns in periplatform carbonates: marginal setting versus glacio-eustacy. *Sed. Geol.*, **175**, 99–113.

Schlager, W. and **Camber, O.** (1986) Submarine slope angles, drowning unconformities and self-erosion of limestone escarpments. *Geology*, **14**, 762–765.

Schlager, W., Reijmer, J.J.G. and **Droxler, A.W.** (1994) Highstand shedding of carbonate platforms. *J. Sed. Res.*, **64**, 270–281.

Stuiver, M. and **Reimer, P.J.** (1993) Extended ^{14}C database and revised CALIB radiocarbon calibration program. *Radiocarbon*, **35**, 215–230.

Tomczak, M. and **Godfrey, J.S.** (2003) *Regional Oceanography: An Introduction*. Daya Publishing House, Delhi, 390 pp. Available at: www.es.flinders.edu.au/~mattom/regoc/pdfversion.html.

Tournadour, E., Mulder, T., Borgomano, J., Hanquiez, V., Ducassou, E. and **Gillet, H.** (2015) Origin and architecture of a Mass Transport Complex on the northwest slope of Little Bahama Bank (Bahamas): relations between off-bank transport, bottom current sedimentation and submarine landslides. *Sed. Geol.*, **317**, 9–26.

Webster, J.M., Braga, J.C., Clague, D.A., Gallup, C., Hein, J.R., Potts, D.C., Renema, W., Riding, R., Riker-Coleman, K., Silver, E. and **Wallace, L.M.** (2009) Coral reef evolution on rapidly subsiding margins. *Global Planet. Change*, **66**, 129–148.

Wilson, M.E.J. and **Vecsei, A.** (2005) The apparent paradox of abundant foramol facies in low latitudes: their environmental significance and effect on platform development. *Earth Sci. Rev.*, **69**, 133–168.

Wunsch, M., Betzler, C., Lindhorst, S., Lüdmann, T. and **Eberli, G.P.** (2016) Sedimentary dynamics along carbonate slopes (Bahamas archipelago). *Sedimentology*. doi:10.1111/sed.12317.

